J. Inst. Eng. India Ser. B (March–May 2013) 94(1):61–69
DOI 10.1007/s40031-013-0042-3

A CASE STUDY

Design, Analysis and Implementation of a Small Signal Control Strategy on a 10 kVA STATCOM Prototype Connected to Inductive Load

J. K. Moharana · M. Sengupta · A. Sengupta

Received: 14 October 2012 / Accepted: 13 February 2013 / Published online: 31 August 2013

Abstract Power factor on the supply side at point of common connection (PCC) can be improved through reactive power compensation using a static synchronous compensator (STATCOM). This approach is becoming increasingly popular in power system applications. In this paper, a small signal model of the STATCOM is practically implemented for maintaining unity power factor on the grid side in presence of inductive loads using a 10 kVA laboratory prototype. The designed controller is first simulated and then experimentally validated on the above laboratory prototype. Excellent agreement between the simulated and experimental results demonstrates the effectiveness of the proposed control strategy and highlights the accuracy of the experiments.

Keywords FACTS · VSI · STATCOM · Small signal model · dc-link pre-charge

Introduction

The ever increasing volt ampere (VA) loading on electric power lines has resulted in an increased need for reactive power compensation. The construction of new power generating stations and transmission networks are facing difficulties due to resource limits, environment issues, right-of-way, cost and other important social issues. This situation has necessitated a review of the traditional power system concepts and practices to achieve greater operating flexibility. The concept of reactive power compensation embraces wide and diverse fields of both system and customer problems, especially related with power factor improvement [1, 2]. Traditionally, rotating synchronous condensers and fixed or mechanically switched capacitors or inductors have been used for reactive power compensation [3]. However, in recent years, static volt ampere reactive (VAR) compensators employing thyristor switched capacitors and thyristor controlled reactors (to inject or absorb the required reactive power) have been developed. Also, the use of self-commutated pulse width modulation (PWM) converters with an appropriate control scheme permits the implementation of static compensators with a time response faster than the fundamental power cycle.

Based on the use of reliable high-speed power electronics device-based self-commutated converters [4–20], many high performance power system controllers have been implemented viz., Static Synchronous Compensator (STATCOM), the Static Synchronous Series Compensator (SSSC) and the Unified Power Flow Controller (UPFC). The STATCOM is in principle a solid-state voltage source converter (with a passive dc-link), connected in parallel to the power system through an ac side reactor. It is analogous to a synchronous condenser. It has no mechanical inertia.

In this paper, first, a popularly accepted mathematical model is derived for the STATCOM and its open loop characteristics demonstrated. Then, the control strategy of the small signal model which has been proposed in [18] is described. The controller for this model has also been derived. This model has been simulated with designed controller by variation of pre-charge voltage on dc-link of the STATCOM. The entire scheme is then validated on a

J. K. Moharana (✉) · M. Sengupta · A. Sengupta
Department of Electrical Engineering, Bengal Engineering and Science University, Shibpur, Howrah, West Bengal, India
e-mail: jkrushna@gmail.com

fabricated prototype. Finally, simulation and experimental results are presented to demonstrate the accuracy and practical feasibility of the scheme. The role of the paper is to experimentally demonstrate/validate the usually adopted model of the STATCOM.

Operating Principles

The operating principles of the STATCOM can be explained by considering the per-phase fundamental equivalent circuit of the STATCOM system as shown in Fig. 1a. An equivalent voltage source is connected to the ac mains through a reactor L_s having a resistance R_s representing the total losses in the inductor, including the converter. If the fundamental component of the output voltage of the STATCOM is in-phase with the supply voltage then the current flowing out or towards the STATCOM is always 90° lagging or leading to the supply voltage as given in Fig. 1b. The STATCOM can also operate, when terminal voltage (fundamental) of the STATCOM is greater than the supply and lagging (and then current will lead the supply voltage). The STATCOM will then operate in fully capacitive mode supplying reactive power of the system. In case STATCOM current lags the system voltage, the STATCOM will operate in inductive mode injecting reactive VARs into the system. This is shown in Fig. 1c. By controlling the phase angle α of the STATCOM terminal voltage with respect to the phase of the source voltage, the dc-link capacitor voltage can be changed and hence the amplitude (of the fundamental component) of the STATCOM terminal voltage can be controlled. In other words, the reactive power either generated or absorbed by the STATCOM can be controlled only by one parameter—the phase angle between the STATCOM output voltage and the supply voltage.

System Modelling

The schematic diagram of STATCOM is shown in Fig. 2. The primary modelling of the STATCOM has been presented by the authors [13–18] using $(d-q)$ transformation. However, for easy reference, the modelling of the above is briefly revisited here. The 3-phase grid voltage, $v_{s,abc}$ lagging with the phase angle difference 'α' to the STATCOM converter terminal voltages $v_{o,abc}$ can be expressed as

$$v_{s,abc}(t) = \begin{bmatrix} v_{sa}(t) \\ v_{sb}(t) \\ v_{sc}(t) \end{bmatrix} = \sqrt{\frac{2}{3}} V_s \begin{bmatrix} \sin(\omega_1 t - \alpha) \\ \sin(\omega_1 t - \frac{2\pi}{3} - \alpha) \\ \sin(\omega_1 t + \frac{2\pi}{3} - \alpha) \end{bmatrix} \quad (1)$$

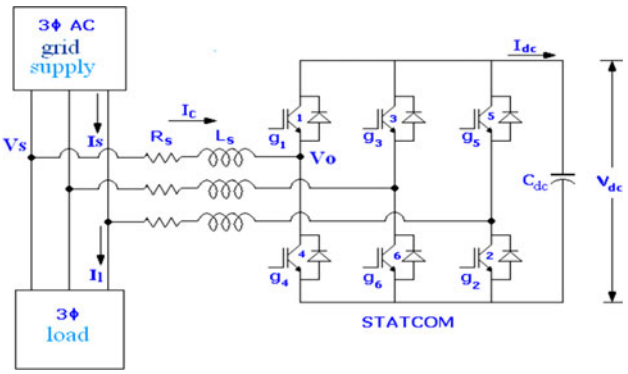

Fig. 2 Simplified main circuit diagram of the STATCOM

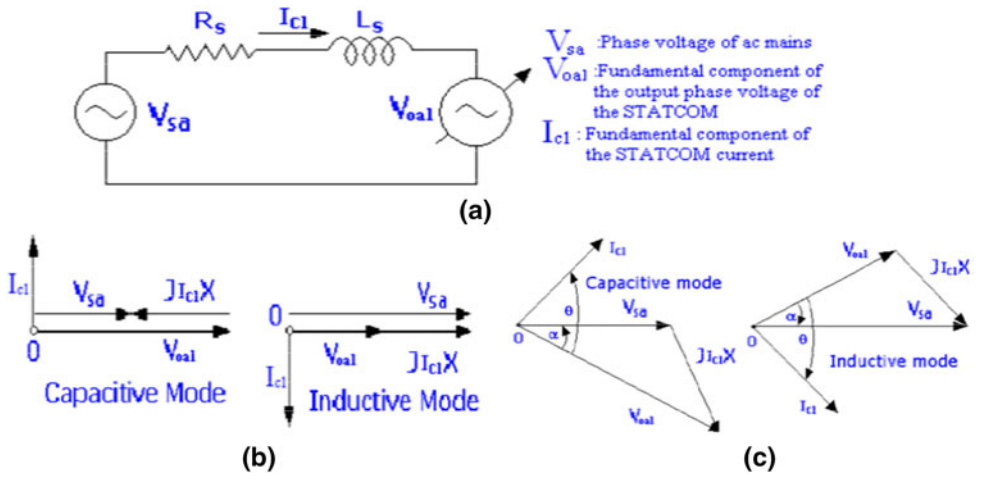

Fig. 1 **a** Per-phase fundamental equivalent circuit, **b** phasor diagram for operation of STATCOM in both modes in-phase and **c** capacitive mode as $\alpha < 0$ and inductive mode as $\alpha > 0$

In the $(d-q)$ reference frame of (1) is

$$v_{s,dqo}(t) = Kv_{s,abc}(t) = V_s[\cos\alpha \quad -\sin\alpha \quad 0]^{\mathrm{T}} \tag{2}$$

where

$$K = \sqrt{\frac{2}{3}}\begin{bmatrix} \sin(\omega_1 t) & \sin\left(\omega_1 t - \frac{2\pi}{3}\right) & \sin\left(\omega_1 t + \frac{2\pi}{3}\right) \\ \cos(\omega_1 t) & \cos\left(\omega_1 t - \frac{2\pi}{3}\right) & \cos\left(\omega_1 t + \frac{2\pi}{3}\right) \\ \frac{1}{\sqrt{2}} & \frac{1}{\sqrt{2}} & \frac{1}{\sqrt{2}} \end{bmatrix} \tag{3}$$

The relationship between the grid voltage and the STATCOM current $i_{c,abc}$, in the series inductor, L_s, in $(d-q)$ reference frame is given by,

$$L_s\frac{\mathrm{d}}{\mathrm{d}t}\left(i_{cd(t)}\right) = \omega_1 L_s i_{cq}(t) - R_s i_{cd}(t) + v_{sd}(t) - v_{od}(t) \tag{4}$$

$$L_s\frac{\mathrm{d}}{\mathrm{d}t}\left(i_{cq}(t)\right) = \omega_1 L_s i_{cd}(t) - R_s i_{cq}(t) + v_{sq}(t) - v_{oq}(t) \tag{5}$$

The STATCOM converter terminal voltages in $(d-q)$ reference frame are given by

$$v_{o,dq} = m_c[1 \quad 0]^{\mathrm{T}} v_{dc}(t) \tag{6}$$

The dc side capacitor current of the STATCOM in $(d-q)$-axes given by (7)

$$i_{dc}(t) = m_c[1 \quad 0][i_{cd}(t) \quad i_{cq}(t)]^{\mathrm{T}} \tag{7}$$

The complete mathematical model of the STATCOM in $(d-q)$ reference is given in (8)

$$\frac{\mathrm{d}}{\mathrm{d}t}\begin{bmatrix} i_{cd(t)} \\ i_{cq}(t) \\ v_{dc(t)} \end{bmatrix} = \begin{bmatrix} -\frac{R_s}{L_s} & \omega_1 & -\frac{m_c}{L_s} \\ -\omega_1 & -\frac{R_s}{L_s} & 0 \\ \frac{m_c}{C_{dc}} & 0 & 0 \end{bmatrix}\begin{bmatrix} i_{cd(t)} \\ i_{cq}(t) \\ v_{dc(t)} \end{bmatrix} + \frac{V_s}{L_s}\begin{bmatrix} \cos\alpha \\ -\sin\alpha \\ 0 \end{bmatrix} \tag{8}$$

The modulation index is given by,

$$\mathrm{MI} = m = \frac{v_{o,peak}}{v_{dc}} = \sqrt{\frac{2}{3}}m_c$$

where, V_s, ω_1, i_{cd}, i_{cq}, v_{dc} and m_c are the line rms voltage of the grid, frequency, rad/s; d and q-axis current of the STATCOM, dc-link voltage and modulation conversion index.

System parameters:

V_s =415 V, $f = f_1 = 50$ Hz, $\omega = \omega_1 = 314$ rad/s;
R_s =1.0 Ω, $L_s = 5.44$ mH, $C_{dc} = 680$ μF, $m = 0.866$, 1.0,
m_c =0.979, 1.2, $R_l = 23\,\Omega$, $L_l = 60$ mH

Open Loop Response

From the mathematical model obtained in (8), the steady state response and transient responses of the STATCOM are presented in [13, 14]. However, the steady state and transient responses are re-plotted with the system parameters given above for further analysis. The steady states values of I_{cq} (steady state q-current) and Q_c (steady state reactive power) (Fig. 3a, b, respectively) are 72 A and −29.4 kVAR for $\alpha = -10°$, respectively. The corresponding transient responses (Fig. 3c, d), in capacitive mode, have high transients. The high transient magnitude of i_{cq} unnecessarily increases the ratings of the STATCOM devices and hence closed-loop control is needed.

Control Strategy

The state space modelling of the STATCOM is given in Eq. (8). It is found to be non-linear in α. Here the control task taken up is to keep m (m_c) constant since α is related to q_c of the STATCOM. This control task is best achieved through small signal model of the STATCOM. The active power (losses plus change of steady state) is indirectly controlled by controlling the dc-link voltage. It may be noted that a single controller is able to perform the control task.

Plant Modelling for Design of Controller

The STATCOM state space model shown in Eq. (8) has been linearized in small signal method [21] and the small signal model is given in Eq. (9). The linearized states $i_{cd\Delta}$, $i_{cq\Delta}$ and $v_{cd\Delta}$ are changes in the reactive component of the current, active component of the current and the dc-link voltage, respectively.

$$\frac{\mathrm{d}}{\mathrm{d}t}\begin{bmatrix} i_{cd\Delta} \\ i_{cq\Delta} \\ v_{dc\Delta} \end{bmatrix} = \begin{bmatrix} -\frac{R_s}{L_s} & \omega_1 & -\frac{m_c}{L_s} \\ -\omega_1 & -\frac{R_s}{L_s} & 0 \\ \frac{m_c}{C_{dc}} & 0 & 0 \end{bmatrix}\begin{bmatrix} i_{cd\Delta} \\ i_{cq\Delta} \\ v_{dc\Delta} \end{bmatrix} + \frac{V_s}{L_s}\begin{bmatrix} -\sin\alpha_\Delta \\ -\cos\alpha_\Delta \\ 0 \end{bmatrix}(\alpha_\Delta) \tag{9}$$

$$Q_{c\Delta} = [-V_S\sin\alpha_\Delta - V_S\cos\alpha_\Delta 0]\begin{bmatrix} i_{cd\Delta} \\ i_{cq\Delta} \\ v_{dc\Delta} \end{bmatrix} + \left[-\frac{(V_S\sin\alpha_\Delta)^2}{R_S}\right]\alpha_\Delta$$

The transfer function relating the reactive power $Q_{c\Delta}$ to the variation in angle α_Δ is found to be

$$P_q(s) = \frac{Q_{c\Delta}}{\alpha_\Delta} = \hat{C}\left[sI - \hat{A}\right]^{-1}\hat{B} + \hat{D} \tag{10}$$

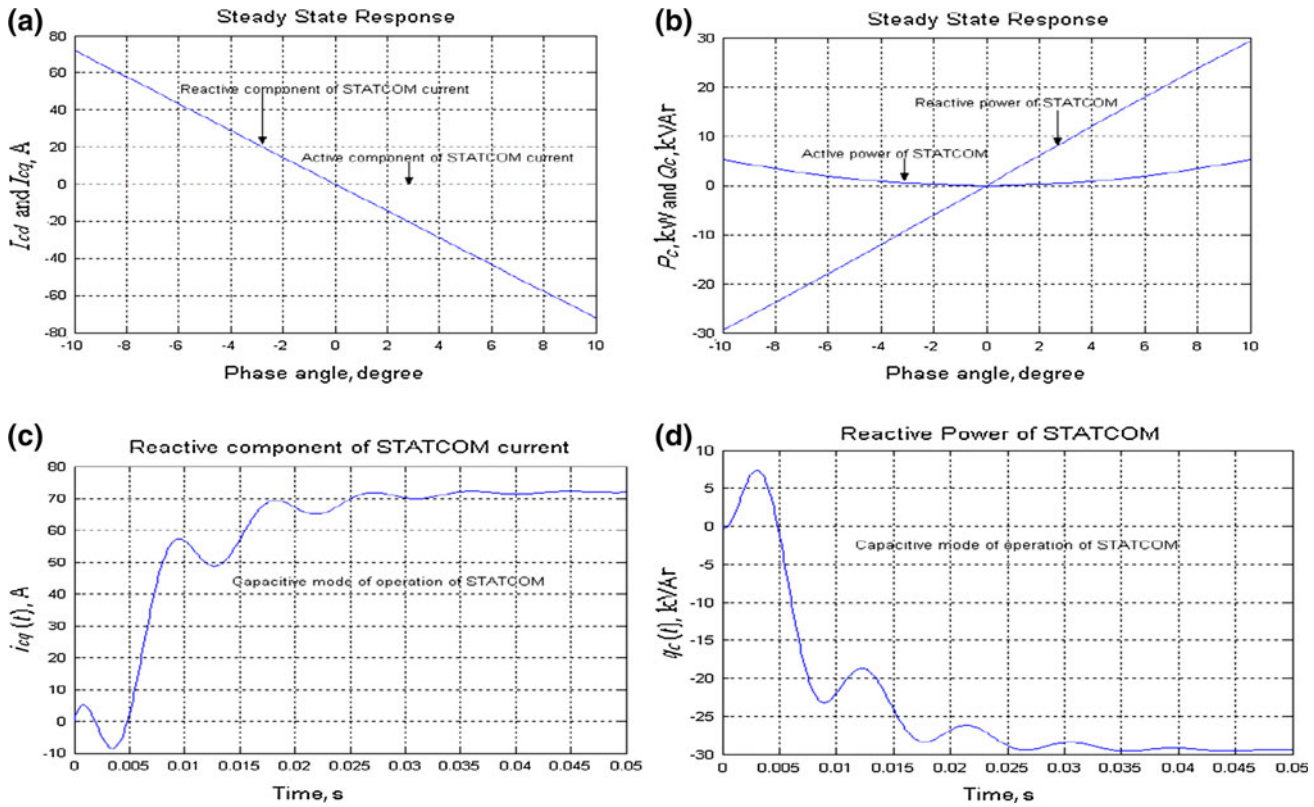

Fig. 3 Responses of the STATCOM for step input: **a** steady state response of α variation plot of I_{cq} with I_{cd}, **b** steady state response of α variation plot of P_c with Q_c, **c** transient responses of time variation plot of i_{cq} in capacitive mode and **d** transient responses of time variation plot of q_c in capacitive mode

The open loop response of the STATCOM with the variations of α ($\alpha_\Delta = 0°$ and $\alpha_\Delta = -10°$) is shown in Fig. 4. In both the cases, the output of the STATCOM (reactive VAR) is much larger than the designed values. Hence, closed loop control is attempted.

Design of Power Controller

PI controller has been designed [13] and given in Eq. (11)

$$K_p = K_q = 7.5 \times 10^{-6}\text{rad/var}$$
$$K_i = \frac{K_q}{\tau} = 2.5 \times 10^{-3}\,\text{s/var} \quad (11)$$

The responses of closed loop system along with PI-controller are shown in Fig. 5.

Proposed Control Strategy

The control strategy is shown in Fig. 6. The injected q_c is summed with the q_c^* (demanded by the load). The error signal is passed through the PI-controller as given in Eq. (11). The output of the controller generates α. Three-phase of the STATCOM output voltages are generated by 120° apart from each other with the angle summing of the phase angle α and synchronizing θ from PLL [22]. Then 3-phase

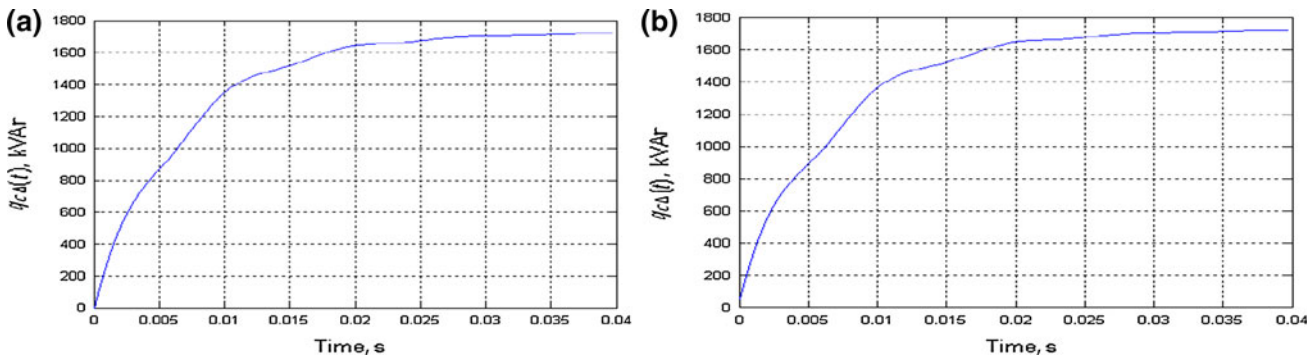

Fig. 4 Open loop response of $q_{c\Delta}$: **a** for $\alpha_\Delta = 0°$, **b** for $\alpha_\Delta = -10°$

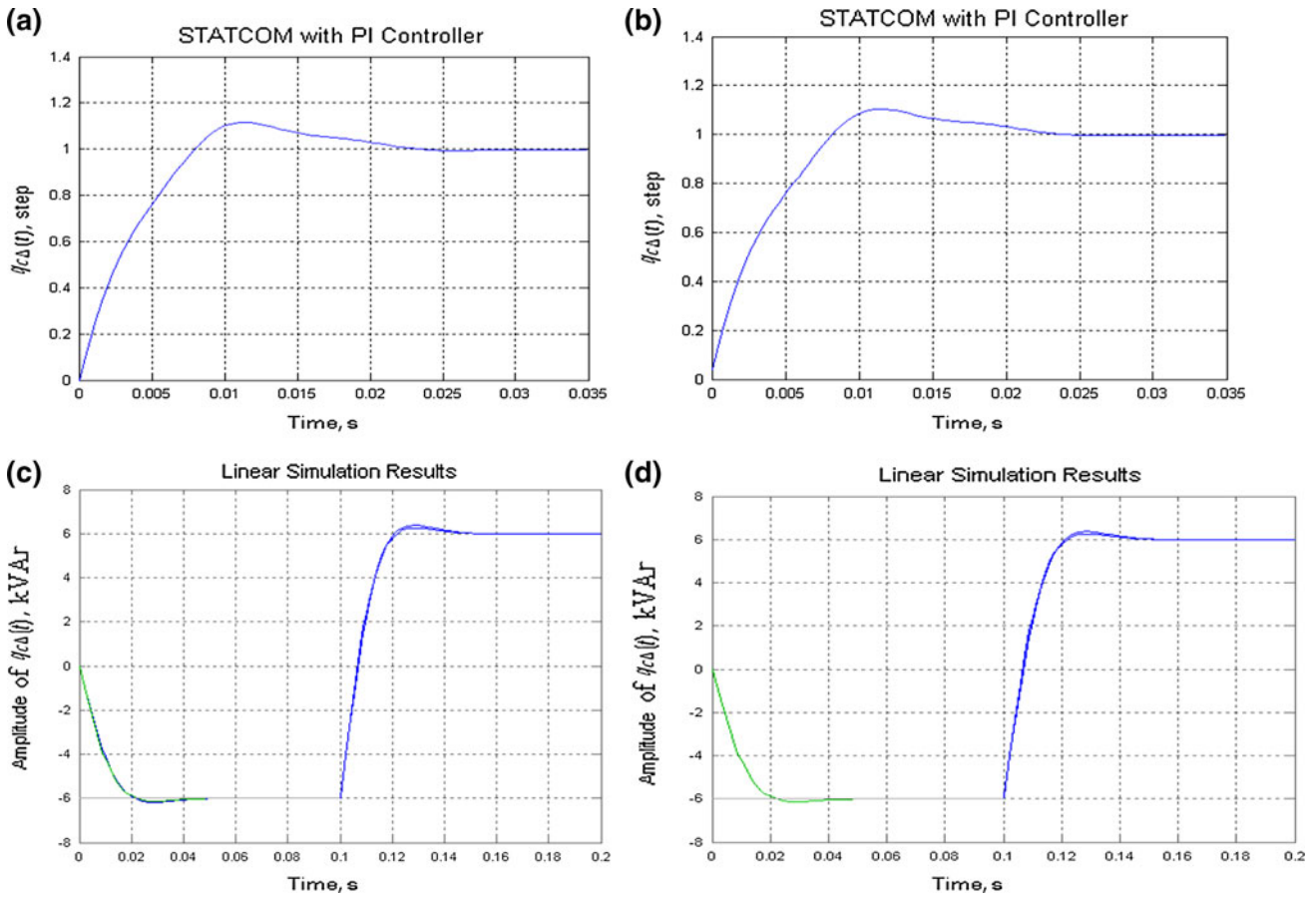

Fig. 5 Closed loop responses of the STATCOM: **a** step response for $\alpha_\Delta = 0°$, **b** step response for $\alpha_\Delta = -10°$, **c** step response with reference of reactive power for $\alpha_\Delta = 0°$ and **d** step response with reference of reactive power for $\alpha_\Delta = -10°$

reference voltages of the STATCOM are generated by multiplying the peak value of the grid voltage and m (M_c). The six pulses for the switching devices of the STATCOM are generated after transforming 3-phase voltages of the terminal voltages of the STATCOM to α–β stationary variables and then six pulses are generated using the principle of space vector pulse width modulation (SVPWM). The scheme is implemented as entire block diagram given in Fig. 7. Though the scheme exists [13] a practical implementation on hardware is done here.

Simulation Results

Simulation of the Linear Load

The linear load is simulated and shown in Fig. 8 here. It may be mentioned that here and elsewhere (unless otherwise mentioned) that voltage is plotted to a reduced scale of 10:1. It is seen that the power factor angle of the grid current (so that pf = 0.77) is 39.64°.

Simulation of the Proposed Strategy

The initial dc-link voltage (pre-charge) of the STATCOM is significant to its transient performance. Hence, the model of the STATCOM (parameters given) is simulated here for different values of the dc-link pre-charge voltage.

Assuming a Pre-charge Voltage of 100 V

The controller works well and STATCOM functions properly for a pre-charge of 100 V on dc-link as shown in Fig. 9a of grid v_{sa} and i_{sa}. It reveals that the STACOM improves the power factor of the grid current after one power cycle at the expense of large transient surge current. The transient variations of all the relevant results at this pre-charge voltage on dc-link are not within the permissible limits for design of the practical set-up of the STATCOM.

Assuming a Pre-charge Voltage of 550 V

The pre-charge voltage on dc-link is increased to 550 V and dynamics of grid v_{sa} with i_{sa} and dc-link are shown in

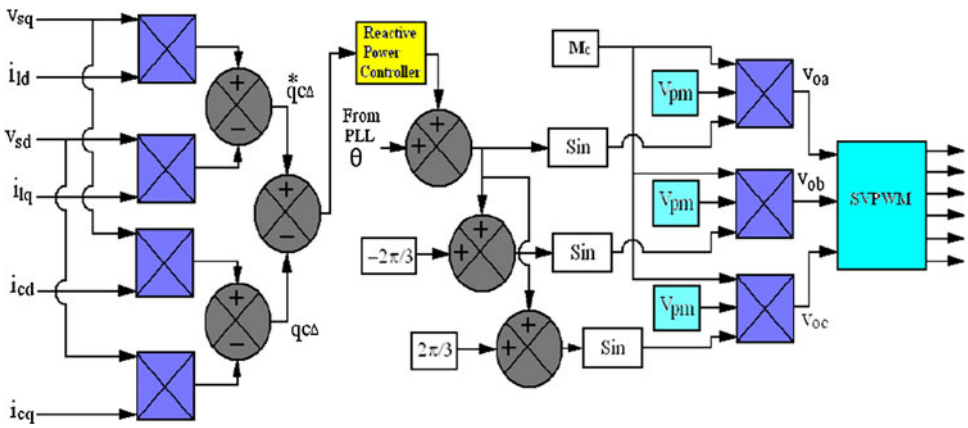

Fig. 6 Closed-loop control strategy

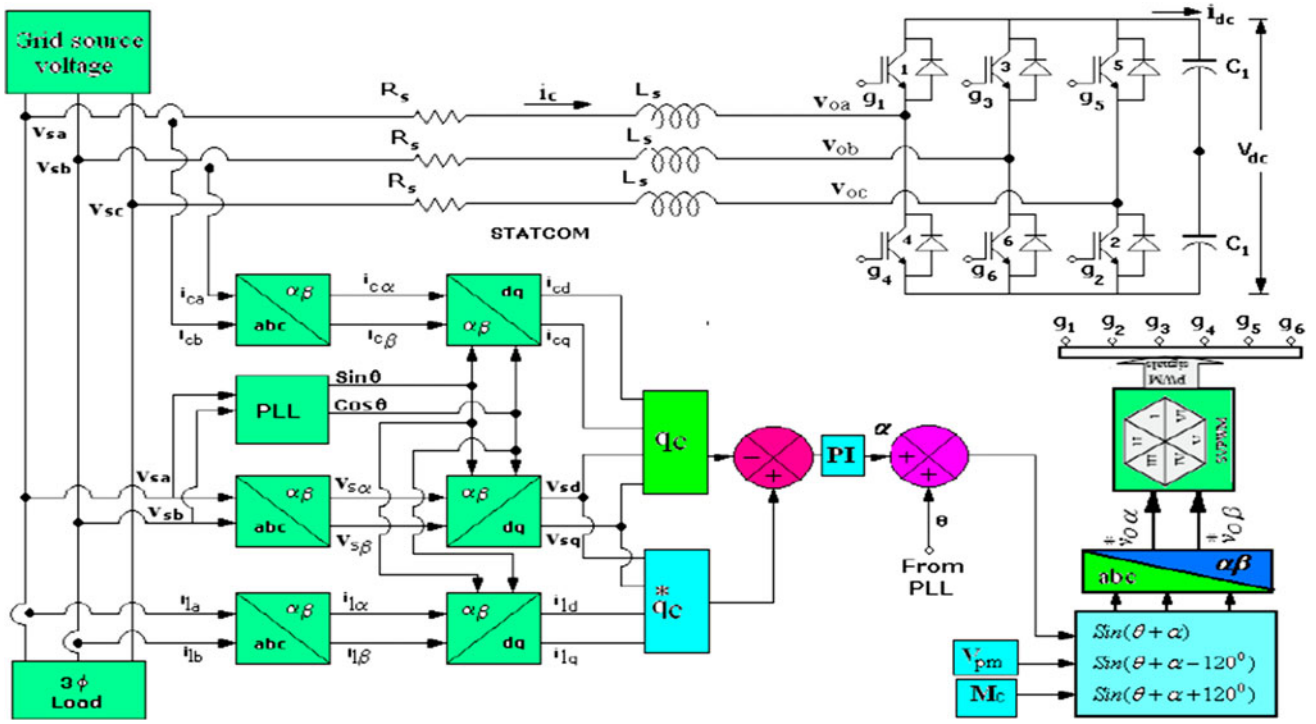

Fig. 7 Implementing diagram

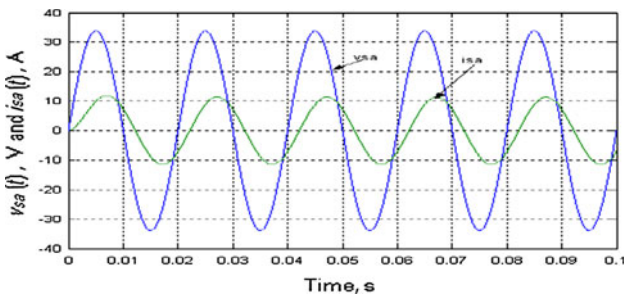

Fig. 8 Grid phase-a voltage and current with *R–L* load before operation of STATCOM

Fig. 9b, c. This depicts that power factor improves but with large enough current spike but dc-link voltage nicely settles at around 660 V.

Assuming a Pre-charge Voltage of 600 V

With further increase in the pre-charge voltage to 600 V, the controller works well with a very small current spike of 15 A (Fig. 9d). It depicts that the improvement of power factor of the grid current takes place in half a power cycle over that given in Fig. 8. Other waveforms are omitted for brevity but their transient variations and settling times are

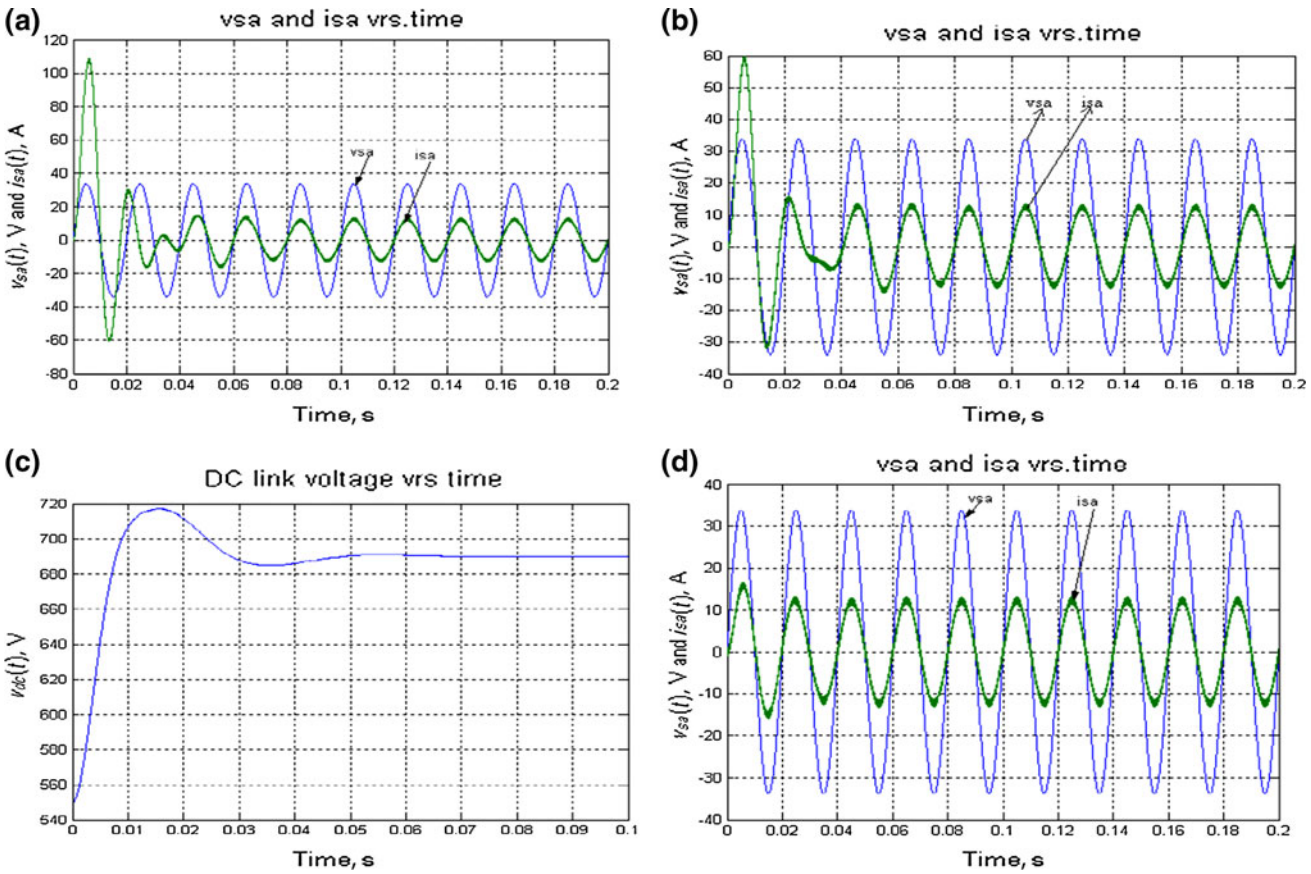

Fig. 9 Simulated responses with different pre-charge voltage: (a) $v_{sa}$with $i_{sa}$for 100 V, (b) $v_{sa}$with $i_{sa}$for 550 V, (c) $v_{dc}$for 550 V and $v_{sa}$with $i_{sa}$for 600 V

found to be within tolerable limits for design of the laboratory set-up of the STATCOM.

Experimental Results

Here, the practical results for power factor improvement of the grid current by using a STATCOM are presented. The prototype of the STATCOM that is fabricated in the laboratory is shown in Fig. 10a.The industrial version with our specifications and necessary protection co-ordination which was fabricated at Veeral Controls and procured is shown in Fig. 10b. It may be noted that the simulated waveforms for voltage build-up differ very slightly with respect to that presented earlier, as in the modified simulation the author has included the effects of different protection mechanisms to mimic the settings in the actual set-up. The pre-charge voltage is 580 V.

The simulated responses of v_{sa} and i_{sa} are presented in Fig. 11a. Figure 11b shows the corresponding experimental waveforms. It is observed that v_{sa} and i_{sa} come in-phase after half a power cycle. It indicates that the STATCOM functions

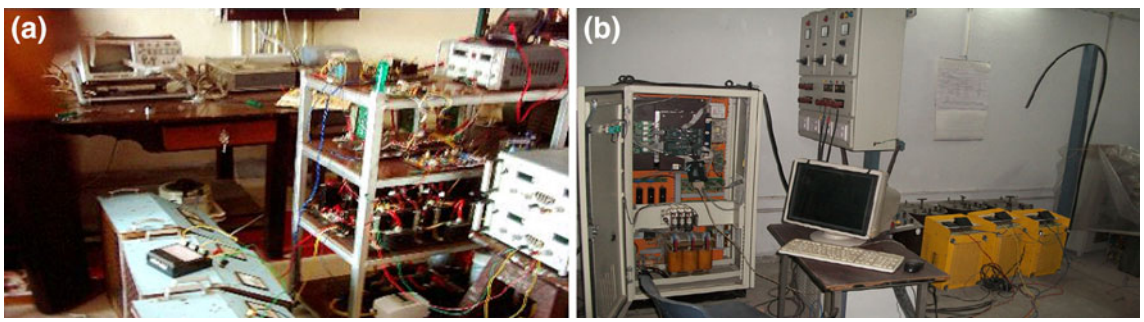

Fig. 10 Fabricated STATCOM **a** laboratory-developed and **b** industrial module. The set-up is existing in the lab premises

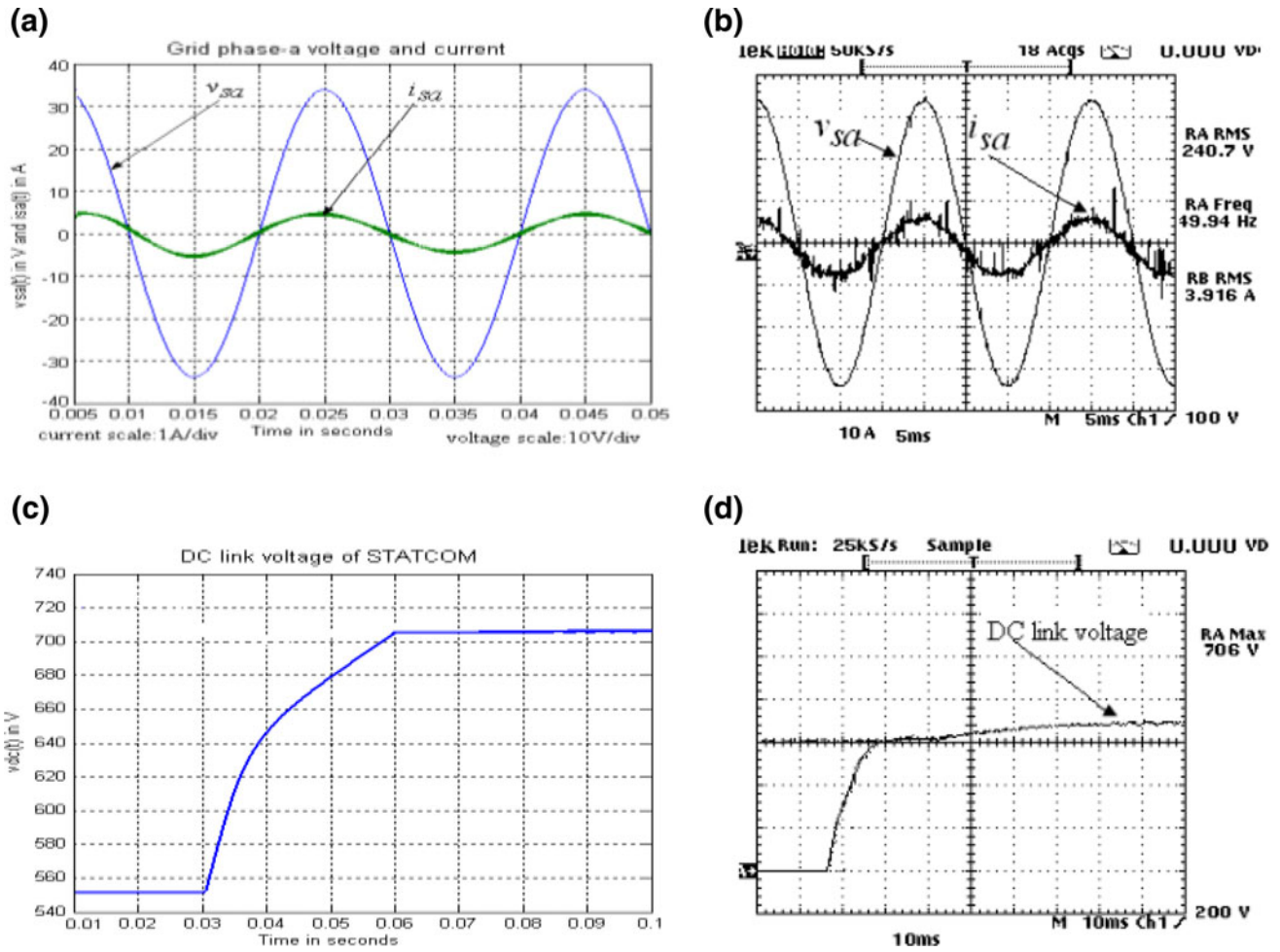

Fig. 11 Simulated and experimental waveforms: **a** Simulated v_{sa} of 240 V (rms) with i_{sa} of 3.89 A (rms), **b** experimental v_{sa} of 240.7 V (rms) with i_{sa} of 3.91 A (rms), **c** simulated v_{dc} rising from pre-charge voltage of 550 V to about 707 V and **d** experimental v_{dc} at a steady state value of 706 V

and compensates the reactive power after half a power cycle. The simulated v_{dc} rises to about 706 V from 580 V due to an arrangement of the protection and pre-charge system (Fig. 11c). The experimental trace of v_{dc} is given in Fig. 11d. It settles to a steady state value of about 706 V. The closed-loop system here has been designed in such a way that there is no separate controller to control the dc-link voltage and it is controlled automatically. Excellent correlation is found between experimental and simulation results. Hence, the implementation of the proposed reactive power controller in real time with hardware may be considered to be significant contribution of the present work.

Conclusions

A small signal control strategy for a STATCOM has been presented here for variations of α only. A single controller controls the reactive power. The strategy works well for the power factor improvement of the grid side current with linear loads. The model is simulated in MATLAB/SIMULINK environment. The peak magnitude transient surges are observed and used for the design of a 10 kVA STATCOM prototype. The role of the paper is to experimentally demonstrate/validate the usually adopted model of the STATCOM. Experimental validation for the same is presented in this paper. Excellent correlation is obtained between the simulated and experimental waveforms. The successful hardware realisation of the proposed control strategy is a significant contribution of this work.

Acknowledgments The authors would like to acknowledge the support received from the All India Council for Technical Education (AICTE) as a part of this work is an outcome of an All India Council for Technical Education-Research Promotion Scheme (AICTE-RPS) Project. The support received from National Mission on Power Electronics Technology (NaMPET) project of the Dehradun Institute of Technology (DIT), Government of India and their Nodal Agency, Centre for Development of Advanced Computing (C-DAC), Thiruvanthapuram is also gratefully acknowledged. Very special thanks are due to M/s Veeral Controls Pvt Ltd., Gandhinagar, for their technical support.

References

1. C.L. Wadhwa, *Electrical Power Systems* (Wiley Eastern Ltd, New Delhi, 1983)
2. E.W. Kimberk, *Power System Stability*, vol. I, II, III (Wiley Eastern Ltd, New Delhi, 1995)
3. P.M. Anderson, A.A. Fouad, *Power System Control and sTability* (Iowa State University Press, Ames, Iowa, 1997)
4. Y.H. Song, in *IEE Power and Energy Series*. Flexible AC transmission systems (FACTS) (IEEE Press, London, 1999)
5. N.G. Hinorani, L.G. Yugyi, Understanding FACTS. (IEEE Power Engineering Society, Standard Publishers Distributors, Delhi, 2001)
6. L. Gyugyi, Reactive power generation and control by thyristor circuits. IEEE Trans. Industrial Appl. **IA–15**(5), 521–532 (1979)
7. A.S. Yome, N. Mithulananthan, Comparison of shunt capacitor, SVC and STATCOM in static voltage stability margin enhancement. Int. J. Electr. Eng. **41**(2), 158–171 (2004)
8. Y. Sumi, Y. Harumoto, T. Hasegawa, New static VAR control using force: commutated inverter. IEEE Trans. Power Apparatus Syst. **PAS-100**(9), 4216–4224 (1981)
9. L.T. Moran, P.D. Ziogas, G. Joos, Analysis and design of a three-phase synchronous solid-state VAR compensator. IEEE Trans. Indus. Appl. **25**(4), 598–608 (1989)
10. C. Schauder, H. Mehta, Vector analysis and control of advanced static VAR compensator. IEEE Proc. Gener. Transm. Distrib. **140**(4), 299–306 (1993)
11. G. Joos, L.T. Moran, P.D. Ziogas, Performance analysis of a PWM inverter VAR compensator. IEEE Trans. Power Electr. **6**(3), 380–391 (1991)
12. B.S. Chen, Y.Y. Hsu, A minimal harmonic controller for a STATCOM. IEEE Trans. Indus. Electr. **55**(2), 655–664 (2008)
13. M.H. Rashid, Power electronics hand book, in *Multilevel Converter and VAR Compensation*, ed. by A. Draou, A. Tahri (Academic Press Harcourt Science and Technology Company, Tokyo, 2001), pp. 599–627
14. G.C. Cho, G.H. Jung, N.S. Choi, G.H. Cho, Analysis and controller design of static VAR compensator using three-level GTO inverter. IEEE Trans. Indus. Electr. **11**(1), 57–65 (1996)
15. J.K. Moharana, M. Sengupta, A. Sengupta, in *NPEC2003, IITB*. Study on an advanced static VAR compensator switched from a space vector PWM inverter-analysis, simulation and comparison with the conventional sinusoidal PWM case (2003), pp. 72–78
16. J.K. Moharana, M. Sengupta, A. Sengupta, in *NPEC2005, II-TKGP*. Design and simulation of current controller and voltage controller for a STATCOM application (2005), pp. 312–316)
17. J.K. Moharana, M. Sengupta, A. Sengupta, in *NPEC-2007*. Modelling, analysis and simulation of various control strategies for a 6 kVA STATCOM for reactive power compensation (IISc, Bangalore, 2007)
18. J.K. Moharana, M. Sengupta, A. Sengupta, in *NPEC-2011*. Closed-loop control of a lab-scale STATCOM prototype for reactive power compensation (BESU, Shibpur, Howrah, 2011)
19. P.S. Sensarma, Analysis and development of a distribution STATCOM for power quality compensation. Ph.D. Thesis (Department of Electrical Engineering, IISc, Bangalore, 2000)
20. J.K. Moharana, Design, analysis and DSP-based implementation of various control techniques on a STATCOM prototype. Ph.D. Thesis (Department of Electrical Engineering, BESU, Howrah, 2012)
21. J.H. Mathew, *Numerical Methods for Mathematics Science and Engineering* (PHI Publication, Delhi, 2003)
22. V. Kaura, V. Blasko, Operation of a phase locked loop system under distorted utility conditions. IEEE Trans. Indus. Appl. **33**(1), 58–63 (1997)